TOR-dependent reduction in the expression level of Rrn3p lowers the activity of the yeast RNA Pol I machinery, but does not account for the strong inhibition of rRNA production

Anja Philippi, Robert Steinbauer, Alarich Reiter, Stephan Fath, Isabelle Leger-Silvestre, Philipp Milkereit*, Joachim Griesenbeck* and Herbert Tschochner*

Institut für Biochemie, Genetik und Mikrobiologie, Universität Regensburg, Universitätsstr. 31, 93053 Regensburg, Germany

ABSTRACT

Ribosome biogenesis is tightly linked to cellular growth. A crucial step in the regulation of ribosomal RNA (rRNA) gene transcription is the formation of the complex between RNA polymerase I (Pol I) and the Pol I-dependent transcription factor Rrn3p. We found that TOR inactivation leads to proteasome-dependent degradation of Rrn3p and a strong reduction in initiation competent Pol I–Rrn3p complexes affecting yeast rRNA gene transcription. Using a mutant expressing non-degradable Rrn3p or a strain in which defined endogenous Rrn3p levels can be adjusted by the Tet-off system, we can demonstrate that Rrn3p levels influence the number of Pol I–Rrn3p complexes and consequently rRNA gene transcription. However, our analysis reveals that the dramatic reduction of rRNA synthesis in the immediate cellular response to impaired TOR signalling cannot be explained by the simple down-regulation of Rrn3p and Pol I–Rrn3p levels.

INTRODUCTION

A crucial step in the regulation of ribosome synthesis is the adjustment of ribosomal RNA (rRNA) gene transcription according to changes in the extracellular environment. Production of rRNAs depends on multiple signalling pathways responding to nutrient availability, stress stimuli or mitogen activation (1–3). One *bona fide* target of the intracellular signal transduction pathways is the ribosomal gene transcription apparatus including RNA Pol I and associated transcription factors. Some of them like mammalian UBF, SL1 and Rrn3/TIF-IA were shown to be either affected by mitotic silencing (4,5) or growth regulated by MAP-kinase (6–8) the mTOR- (target of rapamycin) (9–12), JNK- (13) and casein kinase II-pathways (14–16). These studies suggested that site specific phosphorylation of single factors results in either enhanced or reduced formation of Pol I-complexes initiating transcription at the rDNA promoter. Furthermore, rapamycin-dependent inactivation of rRNA synthesis correlated with the dissociation of Rrn3p/TIF-IA from Pol I and with its translocation from the nucleolus to the cytoplasm (12). It was also proposed that UBF association with the transcribed rDNA region might act as an obstacle for the elongating form of Pol I that can be overcome by growth factor-dependent phosphorylation (17). On the other hand, UBF was suggested to play a role in promoter escape (18). Thus, it appears that eukaryotic rDNA transcription can be regulated at many different levels.

Although regulation of rRNA synthesis is an important TOR function and several targets of TOR signalling affecting the Pol I-machinery were proposed, TOR controls ribosome biogenesis also by stimulating transcription of ribosomal protein genes (19–21) and mRNA translation, the latter especially through translation initiation factor 4E-binding proteins and through the S6 kinase (S6K) [see as review (22)]. Whether and how TOR controls these different processes in a coordinated manner is not understood.

In *Saccharomyces cerevisiae*, formation of initiation complexes at the 35S ribosomal DNA (hereafter called rDNA, rRNA gene) promoter depends on the cooperate activity of upstream activating factor (UAF) with TATA-binding protein, core factor (CF) and initiation competent Pol I which is tightly associated with Rrn3p [reviewed in (3,23)]. Availability of the Pol I–Rrn3p complex represents a limiting step to support 35S rRNA gene transcription. In cells grown to stationary phase or treated with rapamycin, which impairs TOR signalling, the amounts of Pol I–Rrn3p complexes were significantly reduced (11,24). In these conditions Rrn3p-dependent recruitment of Pol I to the rDNA promoter is impaired (11). Concordantly, in yeast cells expressing a covalently bound, non-dissociable complex between Rrn3p and Pol I, down-regulation of rDNA transcription is delayed and Pol I occupancy at the rDNA promoter remains high after inactivation of the TOR pathway (25).

We investigated how nutrient deprivation affects rDNA transcription in yeast and found that Rrn3p-levels are rapidly reduced upon TOR inactivation whereas Pol I-levels remain unaffected. Rrn3p is constitutively degraded by the proteasome and Rrn3p levels decrease as soon as synthesis of the protein is derogated. We found that degradation of Rrn3p correlates with the loss of Pol I–Rrn3p complexes and a reduced Pol I occupancy at the 35S rDNA promoter and coding region. To analyse if Rrn3p degradation plays a major role in the down-regulation of rRNA gene transcription in starved cells, we analysed mutant strains in which Rrn3p levels are unaffected upon TOR inactivation. We found that in these cells Pol I–Rrn3p complex formation and Pol I recruitment to rDNA is only marginally impaired by TOR inactivation while growth inhibition and shut-down of the synthesis of mature rRNAs cannot be rescued. By using the Tet-off system to adjust defined Rrn3p levels we demonstrate that decreasing the amount of cellular Rrn3p results in reduced rDNA transcription and growth rate. However, even minimal amounts of Rrn3p support rRNA production and cell growth. We conclude that the almost complete inhibition of ribosome synthesis upon TOR inactivation cannot fully be explained by Rrn3p degradation and thus reduced rDNA transcription initiation.

MATERIALS AND METHODS

Yeast strains, plasmids and media

See Supplementary Data.

Preparation of yeast whole cell extracts

Yeast cells were harvested by centrifugation (3 min, 3000g, 4°C) and washed once with cold $H_2O_{Millipore}$. After suspending the pellets in the same volume of cold lysis buffer [20% (w/v) glycerol, 150 mM HEPES (pH 7.6), 10 mM MgCl$_2$, 400 mM (NH$_4$)$_2$SO$_4$, 5 mM β-mercaptoethanol, 1 mM PMSF, 2 mM benzamidine], cells were broken for 45 min with pre-cooled glass beads (Ø 0.75–1.0 mm, Roth) on a VXR basic Vibrax (IKA) with 2000–2200 r.p.m. at 4°C. The suspensions were mixed with 150–250 μl of cold lysis buffer and glass beads and cell debris were sedimented (15 min, 13 000 r.p.m., 4°C). The supernatants [whole cell extracts (WCEs)] were frozen in liquid nitrogen and stored at −80°C.

Isolation of (poly)ubiquitylated proteins from yeast extracts

WCEs were adjusted to 750 mM KOAc, 0.5% (v/v) Nonidet P40, 0.05% (v/v) Triton X-100 and incubated with recombinant GST-Dsk2p bound to 50 μl glutathione sepharose (GE Healthcare). Dsk2p is an ubiquitin-binding protein. A mock isolation using recombinant GST bound to 50 μl glutathione sepharose (GE Healthcare) served as a control. After batch binding beads were washed twice with 750 mM KOAc, 0.5% Nonidet P40 and twice with PBS. Precipitated proteins were eluted from the beads with SDS sample buffer and analysed by western blotting.

In vivo pulse labelling and northern blot experiments

After harvesting 3–5 ml of yeast cultures, cells were suspended in 1 ml of the respective medium and pulse-labelled for 15 min with 20 μCi [5, 6-^{3}H] uracil (Amersham) at 30°C. Total RNA was isolated by hot-phenol extraction and ethanol-sodium acetate precipitation (26), separated in a denaturing 1.3% agarose gel and transferred onto a nylon membrane (Positive^{TM}, Qbiogene). ^{3}H-labelled rRNAs were visualized using a BAS-MS 2040 imaging plate (Fujifilm) and a BAS 1000 phosphorimager (Fujifilm, 4–5 days exposition). Quantification was performed using the Image Gauge software (Fujifilm).

For northern blot analysis membranes were hybridized with a ^{32}P-labelled 25S oligonucleotide probe (#212: 5′-CTC CGC TTA TTG ATA TGC-3′) using the RadPrime DNA labelling system (Invitrogen) with incorporation of [α-32P]dATP (Hartmann analytic) according to the instructions of the manufacturer. Quantification was performed as described above, but using a BAS-III imaging plate (Fujifilm).

Gelfiltration of yeast WCEs

Yeast WCEs were first clarified by centrifugation (40 min, 100 000g, 4°C). The supernatants (900 μg of protein) were loaded on a Superose® 6 HR 10/30 column (FPLC®, Pharmacia Biotech) and separated in a high salt buffer [10% (w/v) glycerol, 20 mM HEPES (pH 7.8), 2 mM MgCl$_2$, 0.02 mM EDTA, 1.5 M potassium acetate, 0.05% (v/v) Tween 20, 5 mM β-mercaptoethanol, 1 mM PMSF, 2 mM benzamidine] at a flow rate of

0.35 ml/min. Fractions of 500 µl were collected. An amount of 250 µl of every second fraction were TCA precipitated and analysed by western blotting.

Co-immunoprecipitations

To characterize the Pol I–Rrn3p interaction in yeast strains pNOP1-RRN3-Prot.A-RPA43-HA$_3$ and pNOP1-RRN3-ΔN-Prot.A-RPA43-HA$_3$, cells were crosslinked and lysed as described [(27) and below]. The HA$_3$-tagged Pol I subunit A43 was immunoprecipitated from 250 µl of the resulting extracts with 1.5 µg of an anti-HA antibody (3F10, Roche) bound to 50 µl of Protein G sepharose (Amersham). For the following washing steps the chromatin IP washing buffers were used (see below). To elute the immunoprecipitated proteins and to reverse the crosslink, the beads were mixed with SDS sample buffer and incubated for 20 min at 95°C. Fifty percent of the eluates were analysed by western blotting.

To determine the amounts of co-precipitated Rrn3p, both the Rrn3p and the A43 signals were detected with the LAS 3000 imaging system and quantified using the AIDA software (Raytest). Then, the Rrn3p levels were normalized to the A43 levels and the values of the growth arrested cells were related to the values obtained with extracts of growing cells which were put arbitrarily to 100%.

Chromatin immunoprecipitations

Chromatin immunoprecipitations were performed as described (27). An amount of 45 ml yeast cultures (OD$_{600}$ = 1.0) were crosslinked for 15 or 30 min with 1% (v/v) formaldehyde at 30°C. The cells were harvested by centrifugation and suspended in the same volume of cold lysis buffer [50 mM HEPES (pH 7.5), 140 mM NaCl, 1 mM EDTA, 1% (v/v) Triton X-100, 0.1% (w/v) DOC, 1 mM PMSF, 2 mM benzamidine]. Glass beads (Ø 0.75–1.0 mm, Roth) were added and cells were disrupted on a VXR basic Vibrax (IKA) for 45 min with 2000–2200 r.p.m. at 4°C. After discarding the glass beads, the lysates were sonified to obtain an average DNA fragment size of 500–1000 bp. Cell debris was removed from the lysates by centrifugation (20 min, 13 000 r.p.m., 4°C).

The resulting chromatin extracts were incubated for 2 h at 4°C with 1.5 µg of a monoclonal α-HA antibody (3F10, Roche) bound to 50 µl of Protein G sepharose (Amersham) to enrich the HA$_3$-tagged Pol I subunit A43. After immunoprecipitation, the beads were washed three times with lysis buffer (without protease inhibitors), twice with washing buffer I [50 mM HEPES (pH 7.5), 500 mM NaCl, 1 mM EDTA, 1% (v/v) Triton X-100, 0.1% (w/v) DOC] and twice with washing buffer II [10 mM Tris–HCl (pH 8.0), 250 mM LiCl, 1 mM EDTA, 0.5% (v/v) Nonidet P40, 0,5% (w/v) DOC] followed by a final washing step with TE buffer [10 mM Tris–HCl (pH 8.0), 1 mM EDTA]. Immunoprecipitated material was eluted from the beads by incubating the samples for 10 min at 65°C in the presence of 140 µl of buffer TE containing 1% (w/v) SDS. To reverse the crosslink, 120 µl of the eluates (IPs) as well as 40 µl of the chromatin extracts mixed with 80 µl of TE buffer containing 1% SDS (inputs)

were heated over night at 65°C. Then, proteins were digested by mixing the samples with 130 µl of TE buffer containing 1.54 µg/µl Proteinase K (Sigma). After 2 h of incubation at 37°C, DNA was isolated by phenol–chloroform extraction and ethanol-LiCl precipitation. Both, the input and the IP DNA were suspended in 50 µl of TE buffer.

DNA dilutions of 1: 2000 (inputs) and 1: 400 (IPs) were analysed in triplicates by quantitative real-time PCR using a RotorGene RG-3000 system (Corbett Research) and the SYBR Green I dye (Roche) for detection. To characterize the rDNA occupancy of Pol I subunit A43, a rDNA promoter fragment, a part of the 18S and 25S rRNA coding region and a 5S rRNA gene fragment were amplified using the following oligonucleotides: #969 (5′-TCA TGG AGT ACA AGT GTG AGG A-3′) and #970 (5′-TAA CGA ACG ACA AGC CTA CTC-3′), #710 (5′-TGG AGC AAA GAA ATC ACC GC-3′) and #711 (5′-CCG CTG GAT TAT GGC TGA AC-3′), #712 (5′-GAG TCC TTG TGG CTC TGG GC-3′) and #713 (5′-AAT ACT GAT GCC CCC GAC C-3′), #920 (5′-GCC ATA TCT ACC AGA AAG CAC C-3′) and #921 (5′-GAT TGC AGC ACC TGA GTT TCG-3′). Data were evaluated using the comparative quantitation module of the RotorGene analysis software (version 6.1, Corbett Research) and the MS Office program Excel 2003. After normalizing the IP to the respective input values, relative occupancies were obtained by relating data to the promoter occupancy of the growing cells, which was put arbitrarily to 1.0.

Fractionation

Nuclear and cytoplasmic fractions were prepared as described (28) according to the method of (29) with the modification that 12 ml of yeast cultures were grown to an OD of 0.8 before they were harvested.

Psoralen crosslinking analyses

Psoralen crosslinking was carried out as previously described (30).

Southern blot analysis

Blot analysis and quantitation have been performed as described elsewhere (30). Templates for probe preparation, detecting the rDNA locus were an Eco RI fragment spanning nt 323–2277 of the 35S rDNA, and a 3.5 kb Nco I-fragment spanning nt 1045–4491 of the 35S rDNA.

Immunolocalization

Immunofluorescence microscopy was performed according (28).

Specimen preparation for electron microscopy

Yeast chromatin spreading was performed as described in (31).

RESULTS

Reduction of Rrn3p-levels in growth-arrested yeast cells is dependent on the proteasome

We have previously reported that down-regulation of rRNA synthesis in stationary yeast cells coincides with a lower recovery of Pol I–Rrn3p complexes (24). A clear reduction of Pol I–Rrn3p complexes was also observed by us (data not shown) and others when pre-rRNA synthesis was down-regulated by the protein synthesis inhibitor cycloheximide, by nutrient starvation, or rapamycin, an inhibitor of TOR-kinases which mimics conditions of nutrient starvation (32) (11,12,33,34).

This reduction of Pol I–Rrn3p complexes in yeast correlates with decreasing amounts of Rrn3p in whole cell extracts. When exponentially growing yeast strains were either treated with cycloheximide or rapamycin, or depleted in an essential amino acid, Rrn3p levels were rapidly reduced (Figure 1A). After 120 min, Rrn3p-levels dropped below 20% of the initial amount in all three

conditions. A reduced level of Rrn3p is also detectable if Pol II-dependent transcription is inhibited i.e. when a temperature-sensitive RNA polymerase II mutant (rpb1-1) is shifted to the restrictive temperature, or if cells are in stationary phase (data not shown). In contrast, Pol I levels remain rather stable in growth arrested cells (Figure 1A, lower panel, data not shown). This demonstrates that inactivation of both, TOR pathway, and protein synthesis results in a reduction of the Rrn3p protein level.

The rapid down-regulation of Rrn3p in growth arrested cells depends on the proteolytic activity of the proteasome. In a temperature-sensitive mutant which is defective in CIM3/SUG1, a gene coding for an essential subunit of the regulatory 19S subunit of the proteasome (35,36), Rrn3p is stable upon amino-acid depletion at the restrictive temperature (Figure 1B). In contrast, deletion of vacuolar proteases like PEP4 does not affect the reduction in Rrn3p levels after growth arrest (data not shown).
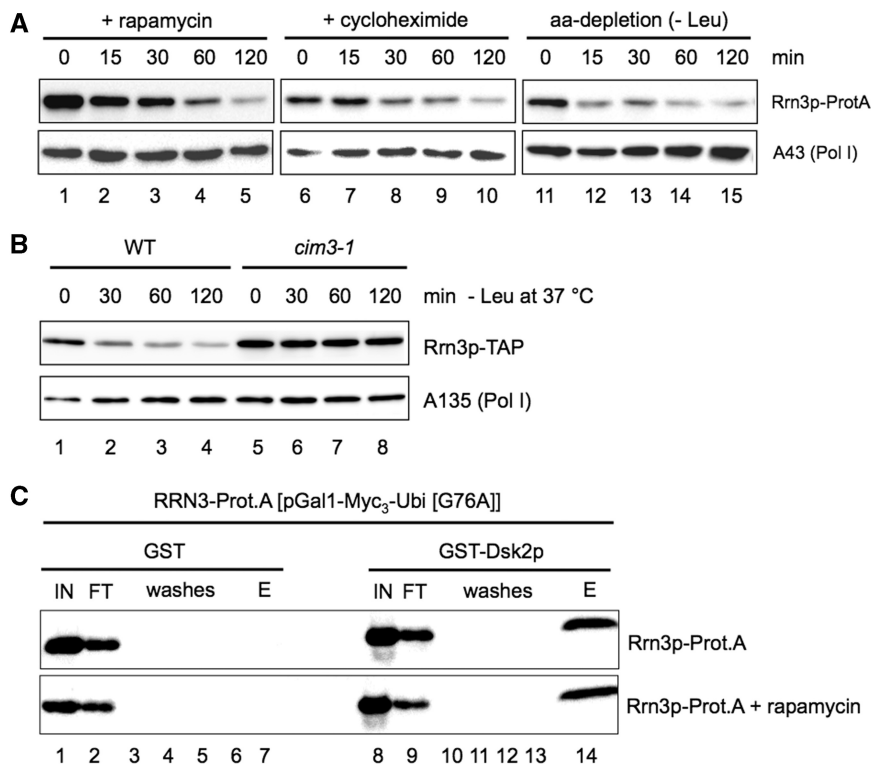

Figure 1. Rrn3p levels are reduced upon TOR inactivation and proteasome-dependent degradation. (**A**) Rrn3p is degraded upon TOR inactivation and inhibition of translation. Yeast strain RRN3-Prot.A expressing a chromosomally Prot.A-tagged Rrn3p was grown in YPD at 30°C to mid-log phase ($OD_{600} \approx 0.4$; $t = 0$ min), before the cells were either treated with 200 ng/ml of rapamycin or with 100 µg/ml of cycloheximide, or starved in SDC-Leu (aa-depletion), respectively. At the time points indicated cells were collected and lysed. Same amounts of WCE (20 µg) were analysed by western blotting using antibodies directed against the Prot.A-tag of Rrn3p and the Pol I specific subunit A43, respectively. (**B**) Rrn3p-degradation depends on proteasome activity. The proteasome ts-mutant strain (*cim3-1, TOY 652*) expressing a chromosomally TAP-tagged Rrn3p or the isogenic *CIM3* WT strain (WT, *TOY 651*) were grown to mid-log phase in YPD at 24°C ($t = 0$ min), before the cells were starved at 37°C in SDC-Leu medium (-Leu). At the time points indicated cells were collected and lysed. Same amounts of WCE (30 µg) were analysed by western blotting using antibodies directed against the TAP-tag of Rrn3p and the Pol I subunit A135, respectively. (**C**) Rrn3p is ubiquitylated. Yeast strain pNOP1-RRN3-Prot.A, expressing Prot.A-tagged Rrn3p from a plasmid was grown in YPD at 30°C to midlog phase, before half of the cells were treated with 200 ng/ml of rapamycin for 10 min. Cells of rapamycin treated and untreated cultures were collected and lysed. Same amounts of WCEs (6 mg) were incubated with either recombinant GST-Dsk2p, or recombinant GST immobilized on 50 µl of glutathione sepharose. After washing, proteins bound to the beads were eluted with SDS sample buffer. Same amounts (1%) (50 µg) of input (IN) and flow through (FT), 0.5% of the wash steps (washes) and 50% of the eluate (E) were analysed by western blotting using antibodies directed against the Prot.A-tag of Rrn3p.

Rrn3p is constitutively ubiquitylated and is rapidly degraded if protein neosynthesis is blocked

To investigate whether Rrn3p-degradation is induced by ubiquitylation we compared ubiquitylation of Rrn3p-Prot.A (WT) before and after inhibition of the TOR pathway. It was previously reported that ubiquitylated proteins can be specifically enriched by their affinity to the immobilized (poly) ubiquitin-binding protein Dsk2p (37). We generated whole-cell extracts from yeast strains expressing Rrn3p-Prot.A before and after 10 min of rapamycin treatment. Rrn3p-Prot.A-containing extracts were incubated with GST (Figure 1C, lanes 1–7) or GST-Dsk2p (Figure 1C, lanes 8–14) fusion protein immobilized on glutathione sepharose. After washings, the GST-baits and associated proteins were eluted and subjected to western blot analysis. Rrn3p-Prot.A was selectively retained by GST-Dsk2p, but not GST alone (Figure 1C and Supplementary Figure S1A, central panel). We also observe specific retention of (poly)ubiquitin and (poly)ubiquitinated proteins on the GST-Dsk2p beads (Supplementary Figure S1A, lower panel). In contrast, binding of the Pol I subunit A135 to immobilized GST-DSK2p in such an experiment was at background level. (Supplementary Figure S1A, upper panel). Rrn3p-Prot.A co-eluting with GST-Dsk2p migrated with slightly lower mobility in SDS–PAGE than Rrn3p-Prot.A in the input and flow-through fractions (Figure 1C, compare lanes 14 with lanes 8 and 9). Even larger Rrn3p-TAP species, likely representing polyubiquitylated Rrn3p-TAP, could be bound to immobilized GST-Dsk2p from extracts of cells expressing the proteasome deficient *cim3-1* mutant and cultured at the restrictive temperature (Supplementary Figure S1B). Interestingly, neither the amount of ubiquitylated Rrn3p-Prot.A bound by Dsk2p nor the extent of polyubiquitylation did increase upon rapamycin treatment (Figure 1C and Supplementary Figure S1B). This suggests that Rrn3p ubiquitylation and proteasome-dependent degradation are not induced upon TOR inactivation. In fact, we observe a strong decrease in RRN3 mRNA levels after 20 min of rapamycin treatment (Supplementary Figure S1C). This is in good agreement with previous transcriptome analyses (38). Thus, the observed decrease of the Rrn3p level is rather due to the inhibition of RRN3 expression and the rapid turnover of the protein.

A C-terminal Prot.A-tagged Rrn3p lacking the 17 N-terminal amino acids is stable upon nutrient starvation

We found a remarkably increased Rrn3p stability in conditions in which TOR is inactive in a strain expressing a C-terminally Prot.A-tagged Rrn3p mutant containing a truncation of the 17 N-terminal amino acids (ΔN) (Figure 2). Deletion of the N-terminal 17 amino acids is required, but not sufficient to inhibit Rrn3p-degradation (data not shown). The C-terminal Prot.A-tag also contributes to Rrn3p-ΔN-Prot.A stability, and accordingly Rrn3p-Prot.A fusion proteins show an increased stability compared to Rrn3p-HA (data not shown). The plasmid-encoded ΔN-mutant fully rescues growth in an *rrn3* deletion strain (Figure 2B). Rrn3p-ΔN-Prot.A levels remained stable even after 2 h of amino acid depletion whereas in this condition about 80% of Rrn3p were degraded in the corresponding reference strain expressing plasmid encoded wild-type Rrn3p-Prot.A (Figure 2C). In our following studies, this mutant served as a tool to investigate how the stability of Rrn3p influences the integrity of the transcription machinery and the synthesis of rRNA in response to nutrient starvation.

Non-degraded yeast Rrn3p keeps its subcellular localization in growth-arrested cells

It has previously been reported that upon TOR-inactivation mammalian Rrn3p/TIFIA translocates from the nucleolus to the cytoplasm (12). Therefore, we
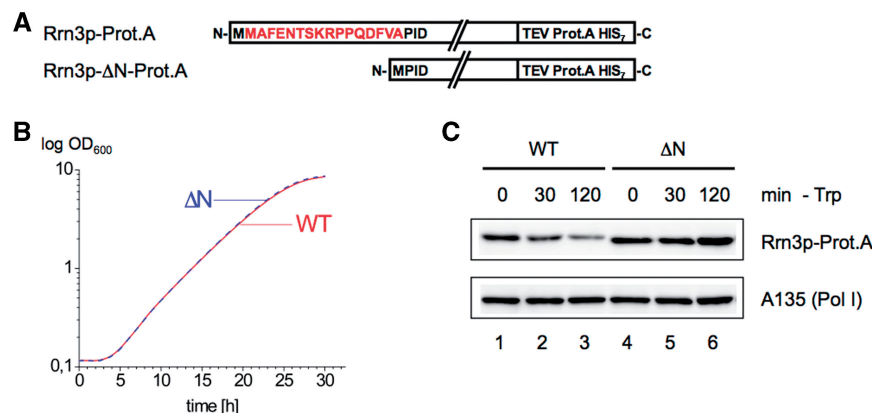

Figure 2. N-terminally truncated Rrn3p-Prot.A (Rrn3p-ΔN-Prot.A) is stable upon TOR inactivation. (**A**) Primary structure of the wild-type protein Rrn3p-Prot.A and the N-terminally truncated version Rrn3p-ΔN-Prot.A. The 16 amino acids deleted in Rrn3p-ΔN-Prot.A are indicated in red. The two fusion proteins are expressed from a centromeric vector under the control of the *NOP1* promoter in a strain deleted in the endogenous *RRN3* locus. (**B**) Growth curves of strains pNOP1-RRN3-Prot.A (WT) and pNOP1-RRN3-ΔN-Prot.A (ΔN) cultured at 30°C in YPD. (**C**) Rrn3p-ΔN-Prot.A resists degradation. Yeast strains pNOP1-RRN3-Prot.A (WT) and pNOP1-RRN3-ΔN-Prot.A (ΔN) were grown in YPD at 30°C to mid-log phase (t = 0 min) and then starved in SDC-Trp (-Trp). At the time points indicated cells were collected and lysed. Same amounts of WCE (30 µg) were analysed by western blotting using antibodies directed against the Prot.A-tag of the Rrn3p versions and the Pol I subunit A135, respectively.

analysed whether a cellular redistribution of Rrn3p after nutrient deprivation occurs also in yeast. Immunolocalization experiments confirmed that Rrn3p disappears rapidly after nutrient starvation in wild-type cells, but neither in the ΔN-mutant (Figure 3A), nor in proteasome-deficient *cim3-1* cells (Figure 3B). Furthermore, in both mutants the nuclear-cytoplasmic distribution of Rrn3p did not change. The amount of cytoplasmic versus nuclear Rrn3p-ΔN-ProtA was also analysed by western blotting after fractionation of whole cells into nuclei and cytoplasm (Supplementary Figure S2). In accordance with the immunolocalization experiments the ratio between nuclear and cytoplasmic Rrn3p was very similar before and after depletion. From these experiments we conclude that the major population of wild-type yeast Rrn3p does not translocate after nutrient depletion.

Maintaining Rrn3p levels upon nutrient depletion preserves the number of Pol I–Rrn3p complexes

We asked how nutrient availability influences formation of Pol I–Rrn3p complexes in wild-type and mutant strains. Many experiments of several groups including ours demonstrated that down-regulation of rDNA transcription correlates with the dissociation of the Pol I–Rrn3p complex in stationary and growth-arrested cells. We have previously reported that Rrn3p is present in three different forms in whole cell extracts of exponentially growing cells (39). The major Rrn3p fraction is monomeric, about 20% are tightly bound to Pol I, whereas the remaining Rrn3p is associated with a high molecular weight complex.

To distinguish between the three forms of Rrn3p we performed gelfiltration experiments with whole cell extracts derived from the Rrn3p-Prot.A wild-type and ΔN mutant strain before and after amino-acid depletion (Figure 4A). In nutrient depleted wild-type cells, Rrn3p is significantly reduced to a similar extent in all three populations (Figure 4A, panels WT). In contrast, in the ΔN-mutant the amounts of Rrn3p in all fractions before and after nutrient depletion are comparable (Figure 4A, panels ΔN), suggesting that in this genetic background Pol I–Rrn3p complexes persist upon growth arrest. Similarly, in the *cim3-1* mutant strain both, the total amount of Rrn3p and the ratio of complexed versus free Rrn3p did not change significantly before and after nutrient depletion (Supplementary Figure S3A, panels *cim3-1*). These results indicate that maintaining Rrn3p levels upon nutrient depletion preserves the number of Pol I–Rrn3p complexes.

To assess the number of Pol I–Rrn3p complexes in the two different genetic backgrounds more quantitatively, co-immunoprecipitation experiments under stringent conditions were performed before and after nutrient depletion (Figure 4B). In extracts from nutrient depleted wild-type cells the amount of Rrn3p-Prot.A co-precipitating with HA-tagged Pol I-subunit A43 is strongly reduced, when compared to co-immunoprecipitation experiments with extracts from cells before nutrient depletion (Figure 4B, compare lane 7 with lane 8). In contrast, when the same experiments were carried out with extracts from the ΔN-strain in which Rrn3p levels are maintained after nutrient depletion, ΔN-Rrn3p-Prot.A association with Pol I was
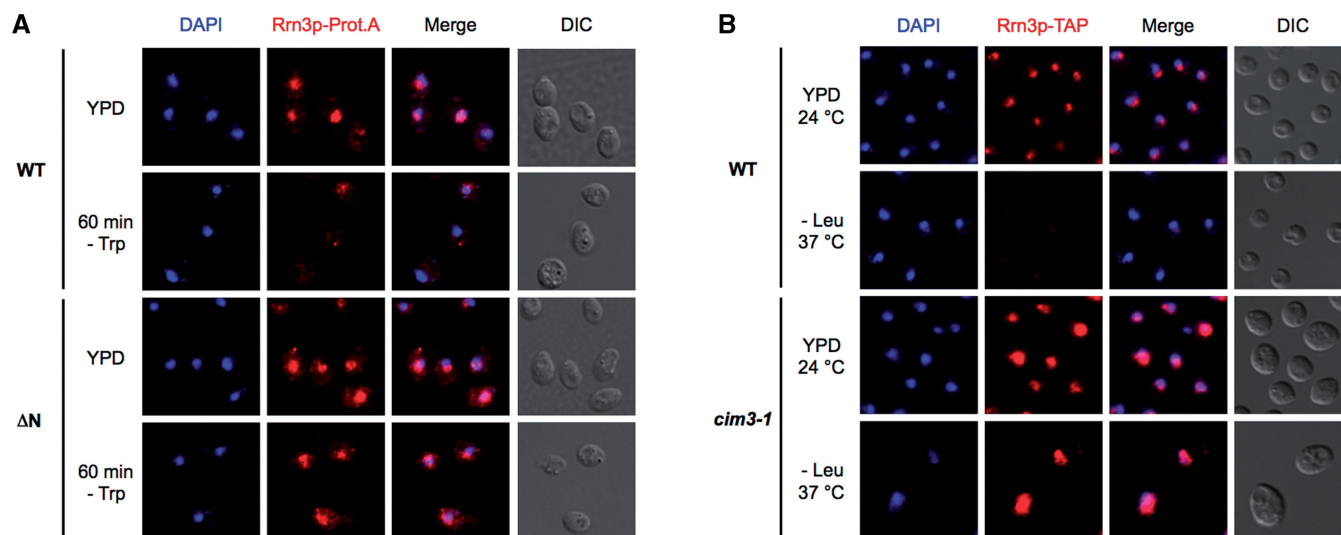

Figure 3. The subcellular distribution of stabilized yeast Rrn3p does not change upon nutrient starvation. (**A**) Immunolocalization. pNOP1-RRN3-Prot.A (WT) and pNOP1-RRN3-ΔN-Prot.A (ΔN) cells either logarithmically growing or after amino-acid depletion were fixed with 4% paraformaldehyde and treated with zymolyase to generate spheroplasts. Anti-protein A antibodies and an Alexa 594-conjugated secondary antibody were used to detect the Prot.A-tagged Rrn3p versions (in red), whereas the DNA was stained with DAPI (in blue). (**B**) Rrn3p-TAP does not change its subcellular localization if proteasome-dependent degradation is inhibited. The proteasome ts-mutant *cim3-1* (TOY 652)(with chromosomally TAP-tagged Rrn3p) and the isogenic WT strain (TOY 651) were grown at 24°C in YPD medium to mid-log phase, before the cells were starved at 37°C in SDC-Leu medium. After 2 h the cells were fixed with 4% paraformaldehyde and treated with zymolyase to generate spheroplasts. TAP-tagged Rrn3p was detected with an α-protein A primary antibody and an Alexa 594-conjugated secondary antibody (in red), while the DNA was stained with DAPI (in blue).
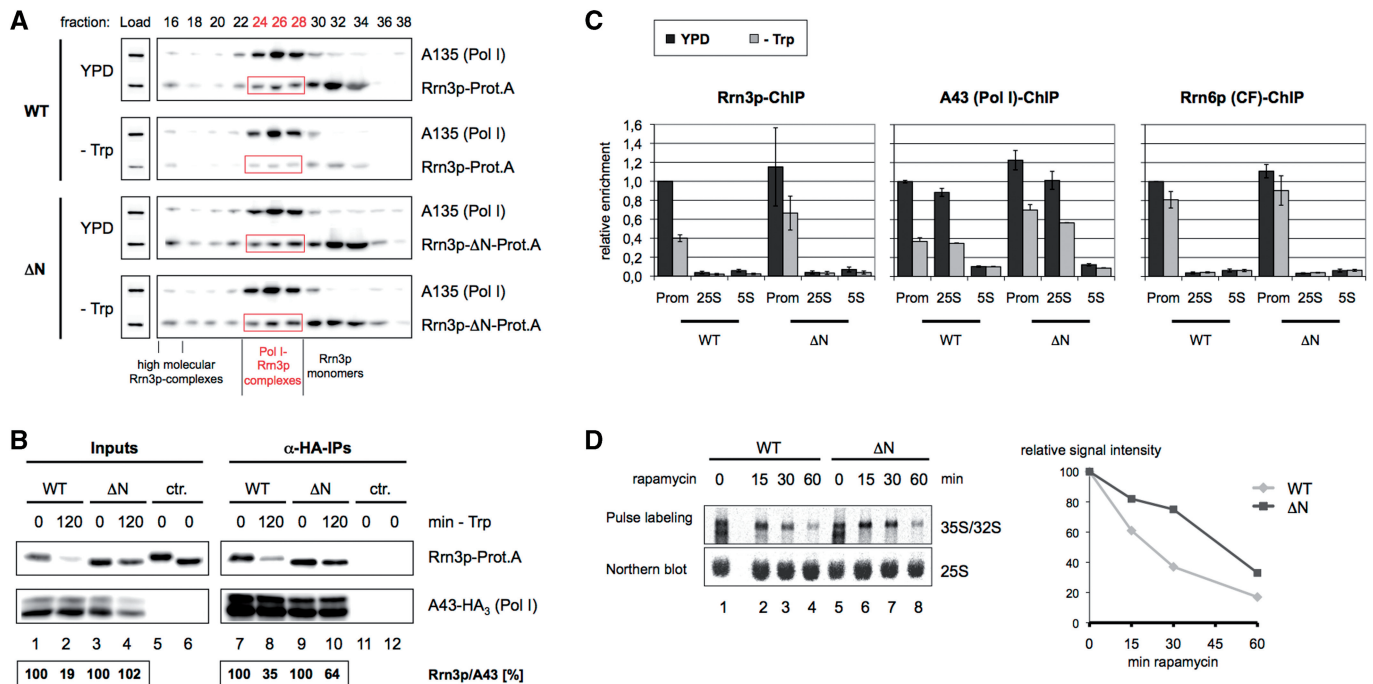
Figure 4. Stabilization of cellular Rrn3p levels attenuates the reduction in initiation competent Pol I–Rrn3p complexes observed upon nutrient depletion. (**A**) Gelfiltration analysis. Yeast strains pNOP1-RRN3-Prot.A (WT) and pNOP1-RRN3-ΔN-Prot.A (ΔN) were grown in YPD at 30°C to mid-log phase. Cells were either starved for 2 h in SDC-Trp (-Trp) or further cultured in YPD and collected by centrifugation. After lysis, same amounts of WCE (900 μg) were separated on a Superose-6® column in a buffer containing 1.5 M potassium acetate. An amount of 250 μl of the collected 500 μl fractions were TCA precipitated and analysed by western blotting together with the 'Load' (30 μg). Antibodies used were directed against the Prot.A-tag of the Rrn3p versions and the Pol I subunit A135, respectively. The gel filtration fractions containing the initiation competent Pol I–Rrn3p complexes are labelled in red. (**B**) Co-immunoprecipitations. Yeast strains TOY 684 (WT) and TOY 685 (ΔN), both expressing chromosomally HA₃-tagged Pol I subunit A43 and either full length or truncated Prot.A-tagged Rrn3p, were grown in YPD at 30°C to mid-log phase and half of the cells was crosslinked with 1% formaldehyde, harvested and lysed (t = 0 min). The remainder of the cells was starved in SDC-Trp (-Trp) for 2 h and treated as described above (t = 120 min). The HA₃-tagged Pol I subunit A43 was immunoprecipitated (α-HA-IPs) from 250 μl of extracts (Inputs) with anti-HA antibody. Fifty percent of the α-HA-IPs as well as 1% of the inputs were analysed by western blotting using antibodies directed against the Prot.A-tag of the Rrn3p versions and the HA-tag of the Pol I subunit, respectively. As a control an identical co-immunoprecipitation experiment was performed using extracts from yeast strain pNOP1-RRN3-Prot.A and pNOP1-Rrn3-ΔN-Prot.A, which do not express the HA-tagged Pol I subunit A43 (ctr.). Western blot signal intensities were measured, and quantified using the LAS 3000 imaging system and the AIDA software. Rrn3p/A43 ratios were calculated, and the ratio of the 120 min samples was normalized to the ratio of the respective 0 min samples which was set to 100%. Numbers calculated are given below each lane. (**C**) Chromatin-IP (ChIP) experiments. Yeast strains pNOP1-RRN3-Prot.A (WT) and pNOP1-RRN3-ΔN-Prot.A (ΔN), both expressing either chromosomally HA₃-tagged Pol I subunit A43 or the core-factor subunit Rrn6p, were grown in YPD at 30°C to mid-log phase and half of the cells was crosslinked with 1% formaldehyde, harvested, lysed and sonified. The remainder of the cells was starved in SDC-Trp for 2 h and treated as described above (-TRP). Rrn3p-Prot.A, the HA₃-tagged Pol I subunit A43 or Rrn6p were immunoprecipitated from the chromatin extracts. After DNA isolation the relative amounts of specific DNA fragments co-purifying with the proteins were measured in triplicate real-time PCR reactions using primers specific for the rDNA promoter (P) and the 25S rRNA coding region (25S) as well as for the 5S rRNA gene (5S) which served as an internal control. Data were normalized to the promoter occupancy in growing wild-type cells and represent the mean of at least three independent ChIP experiments. (**D**) Reduction of 35S pre-rRNA synthesis is attenuated in the ΔN-mutant after TOR inactivation. (Upper panel) Yeast strains pNOP1-RRN3-Prot.A (WT) and pNOP1-RRN3-ΔN-Prot.A (ΔN) were cultured to mid-log phase (t = 0 min), before the cells were treated with 200 ng/ml of rapamycin. At the time points indicated 5 ml of the cultures were pulse labelled for 15 min with 20 μCi of [5, 6-³H] uracil, and total RNA was isolated. Equal amounts of total RNA were separated in a denaturing agarose gel and blotted onto a nylon membrane. ³H-labelled RNAs were visualized and quantified using the BAS 1000 imaging system and the Image Gauge software. To determine the total RNA load per lane the membrane was hybridized with a ³²P-labelled oligonucleotide probe directed against the mature 25S rRNA (northern blot). Radioactive signals were visualized and quantified as described above. (Lower panel) The ratio of nascent 35S precursor rRNA to total 25S rRNA in the different rapamycin treated samples was determined and normalized to the 35S rRNA to 25S rRNA ratio of the untreated sample, which was arbitrarily set to 100.

significantly higher upon TOR inactivation (Figure 4B, compare lanes 9 and 10 with lanes 7 and 8). This result indicates that in nutrient-depleted wild-type cells endogenous Rrn3p-levels and (as a consequence) the number of Rrn3p–Pol I complexes are reduced. On the other hand, some reduction of Rrn3p–Pol I complexes is also observed if TOR is inhibited in the ΔN-mutant. In the experiment depicted in Figure 4B, 64% ΔN-Rrn3p-Prot.A remained bound to Pol I (Figure 4B, lanes 9 and 10), although the

Rrn3p levels are very similar before and after nutrient starvation (Figure 4B, lanes 3 and 4). Similar results were obtained when Rrn3p–Pol I complexes were analysed by co-immunoprecipitation in the *cim3-1* mutant (Supplementary Figure S3B). Accordingly, the reduction of endogenous Rrn3p levels is one important cellular process to decrease the amount of Pol I–Rrn3p complexes, but there are additional mechanisms, which contribute.

Preserving the number of Pol I–Rrn3p complexes attenuates the decrease of Rrn3p and Pol I association with rRNA genes and the shut down of transcription upon nutrient depletion

To investigate whether stable levels of Pol I–Rrn3p complexes in the ΔN-mutant correlate with robust recruitment of Pol I to the rDNA even after inactivation of the TOR pathway, we performed ChIP (chromatin immunoprecipitation) experiments. In good agreement with previous results where TOR signalling was inhibited by the addition of rapamycin (11,40), we observe a decrease of Pol I promoter DNA and DNA fragments of the 35S rRNA coding sequence co-precipitating with Pol I in extracts from wild-type cells being starved of essential amino acids to about 40% of the co-precipitation before starvation (Figure 4C, central panel). The same was observed for Pol I promoter DNA co-purifying with Rrn3p (Figure 4C, left panel). In contrast, in extracts of the ΔN-mutant co-precipitation of the respective rDNA fragments with either Rrn3p or Pol I decreased only to about 60% upon starvation (Figure 4C). Accordingly, the reduction in endogenous Rrn3p levels when nutrients become limiting significantly contributes to but does not fully explain the decreased Pol I loading on rRNA genes in this situation. Nutrient depletion did not lead to significant changes in the association of promoter bound subunits of the transcription factor CF (Figure 4C, right panel) and UAF [data not shown, see also (11)] in wild-type cells and the ΔN-mutant. Thus, CF and UAF remain stably associated with the rDNA promoter upon TOR inactivation although the formation and recruitment of the Pol I–Rrn3p complex is impaired.

Interestingly, the absolute amount of rDNA co-precipitating with Pol I, Rrn3p and CF was modestly increased in the ΔN-mutant. Since only half out of the 150 rRNA genes of the yeast rDNA locus are actively transcribed in wild-type conditions, this could mean that this number is slightly enhanced in strains carrying the mutant *rrn3* allele. Electronmicroscopic inspection of rRNA genes by the Miller chromatin spreading method (41,42) suggested a higher density of actively transcribed rDNA genes in individual nucleolar regions released from ΔN-mutant cells when compared to nucleolar regions released from wild-type cells (Supplementary Figure S4A). To validate the impression obtained in these single-cell analyses, we turned to psoralen crosslinking experiments in which actively transcribed and transcriptional inactive rRNA genes can be distinguished and are averaged over a large cell population (30,43,44). We observed a slight increase (<15%) in the number of actively transcribed rRNA genes in the ΔN-mutant in direct comparison with the corresponding wild-type strain (Supplementary Figure S4B) providing a possible explanation for the increased amount of 35S rRNA gene segments co-precipitating with Rrn3p and Pol I in the mutant strain compared to the corresponding wild-type strain in the above ChIP experiments (Figure 4C).

To investigate how stabilization of Rrn3p levels upon TOR inactivation influences rRNA-production we examined new synthesis of the primary rRNA transcript in the wild-type strain and the ΔN-mutant. We performed pulse labelling experiments with ^{3}H uracil and found that in the wild-type strain, a significant amount of 35S rRNA precursor is still produced after 30 min and even—although to a lower extent—after 60 min of rapamycin treatment (Figure 4D). In the mutant strain expressing Rrn3p-ΔN-Prot.A the ratio of newly synthesized 35S rRNA to steady state 25S rRNA levels is higher at each time-point (up to 2-fold after 30 min of TOR inactivation), when compared to the 35S/25S rRNA ratio in a wild-type strain (Figure 4D, graph on the right) arguing again for a partial deregulation of rDNA transcription in the ΔN-mutant when TOR is inactivated. Taken together these data indicate that (i) after TOR inactivation rDNA transcription is reduced, but still occurs after up to 60 min of rapamycin treatment [see also (11,45)] and (ii) the reduction of endogenous Rrn3p levels under those conditions contributes to the down-regulation of rDNA transcription.

Lowered Rrn3p levels affect Pol I–Rrn3p complex formation, 35S pre-rRNA synthesis and cellular growth, but do not fully mimic the response to TOR inactivation

To uncouple effects of an altered Rrn3p level from other effects mediated by TOR inactivation, we generated a strain in which the only copy of the *RRN3* gene was expressed from a plasmid under the control of a doxycycline repressible 7-fold TetO promoter (pTet$_7$-*RRN3-Prot.A*) (46). Using distinct amounts of doxycycline the expression levels of Rrn3p could be well controlled resulting in a strong down-regulation in the presence of 1 µg/ml doxycycline and a strong overexpression in the absence of the drug (Figure 5A, lanes 1 and 4). Interestingly, the strong decrease in Rrn3p level observed in the presence of 1 µg/ml doxycycline retarded, but did not completely inhibit growth (Figure 5E).

Gelfiltration of whole cell extracts derived from strains in which Rrn3p expression was either enhanced or reduced demonstrated again that Rrn3p levels correlated well with the number of Pol I–Rrn3p complexes (Figure 5B). Thus, changes in the level of Rrn3p did not significantly alter the elution profile of the protein in gelfiltration. This means that a similar ratio of Rrn3p within a given population is monomeric, associated with Pol I, or part of a higher molecular weight complex (compare Supplementary Figure S3A with Figure 4A and Figure 5B). Apparently, there is a cellular mechanism maintaining a fixed ratio between free and complexed Rrn3p.

Next, we wanted to see how rRNA synthesis correlates with pTet$_7$-controlled Rrn3p expression-levels. pTet$_7$-*RRN3-Prot.A* cells were cultured with different amounts of doxycycline and were pulse labelled for 15 min with ^{3}H uracil to monitor rRNA synthesis. We found a significant reduction of newly synthesized rRNA with increasing doxycycline concentrations (Figure 5C). The amount of nascent rRNA levels detected in pulse labelling experiments depends on the one hand on the synthesis of (pre-)rRNA due to Pol I dependent transcription and/or on the other hand, on their turnover due to degradation or productive processing events. Amounts of
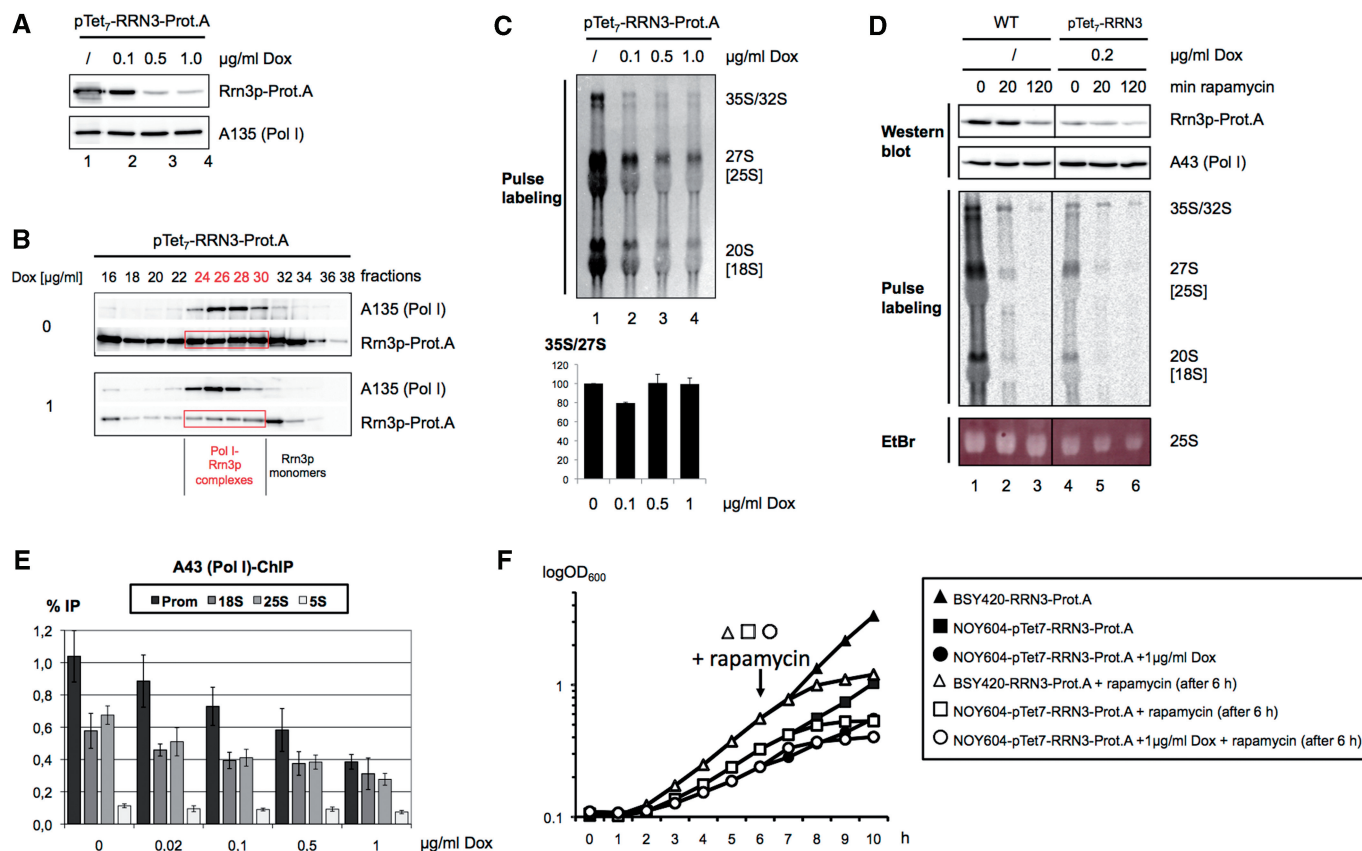
Figure 5. Reduction of Rrn3p-levels decreases rRNA production but does not phenocopy growth-inhibition and the loss of nascent rRNAs upon TOR inactivation. (**A**) Yeast strain pTet$_7$-RRN3-Prot.A (TOY 667), expressing Rrn3p under the control of a doxycycline sensitive 7-fold TetO-promoter was grown in YPAD at 30°C to early log phase, before cells were split and further cultured in the absence or presence of 0.1, 0.5 and 1 µg/ml doxycycline (Dox), respectively. After 17 h, 50 ml of the cultures were collected and lysed and same amounts of WCE (30 µg) were analysed by western blotting, using an antibody directed against the Prot.A-tag of the Rrn3p. (**B**) Overexpression of Rrn3p results in more Pol I–Rrn3p complexes. Yeast strain pTet$_7$-RRN3-Prot.A was grown in YPAD at 30°C without or in the presence of 1 µg/ml doxycycline to log-phase. After lysis, same amounts of WCE (900 µg) were separated on a Superose-6® column and further analysed as described in Figure 4A. Western blots were developed with anti-A135-antibodies which recognize at the same time also Rrn3p-Prot.A through its Prot.A-tag. Note that about equal amounts of Pol I in both strains were detected. The gel filtration fractions in which Rrn3p co-migrates with Pol I are labelled in red. (**C**) Reduction of Rrn3p-levels decreases rRNA synthesis. Five millilitres aliquots of strain pTet$_7$-RRN3-Prot.A growing in the presence of various doxycycline concentrations were pulse labelled for 15 min with 20 µCi of [5, 6-^{3}H] uracil. Twenty percent of the isolated RNA were separated by denaturing gel electrophoresis and blotted onto a nylon membrane. ^{3}H-labelled rRNAs were visualized using the BAS 1000 imaging system and quantified with the Image Gauge software. The graph on the bottom represents the 35S/27S nascent rRNA ratio determined in two separate experiments. The ratio in the 0 µg/ml Dox sample was arbitrarily set to 100. (**D**) Reduction of Rrn3p-levels upon TOR inactivation does not explain the complete shut off of pre-rRNA synthesis. Yeast strain RRN3-Prot.A (WT) expressing a chromosomally Prot.A-tagged Rrn3p was grown in YPD at 30°C to early log phase (t = 0 min). One third of the culture was withdrawn before rapamycin was added to a final concentration of 200 ng/ml and incubation was continued for 20 and 120 min, respectively (t = 20, 120 min). Yeast strain pTet$_7$-RRN3-Prot.A (TOY 667) was grown in YPD in the presence of 0.2 µg/ml doxycycline (Dox) at 30°C for 18 h to early log phase, and treated with rapamycin as described above. From all samples cells from 50 ml were sedimented and WCEs were prepared, from which 30 µg of protein were analysed by western blotting, using an antibody directed against the Prot.A-tag of the Rrn3p. In parallel, 5 ml of the cultures were pulse labelled for 15 min with 20 µCi of [5, 6-^{3}H] uracil and total RNA was isolated. Equal amounts of total RNAs were separated by denaturing gel electrophoresis and visualized by Ethidium bromide staining (EtBr). After transfer onto a nylon membrane ^{3}H-labelled rRNAs were visualized as described in the legend to Figure 5C. (**E**) Chromatin-IP (ChIP) experiments. Yeast strain pTet$_7$-RRN3-Prot.A (TOY 667) was grown in YPD at 30°C to mid-log phase in the presence of the indicated doxycycline concentrations. Cells were crosslinked and analysed as described for Figure 4C. (**F**) Rrn3p expression levels do not influence kinetics of growth inhibition upon TOR inactivation. Strain pTet$_7$-RRN3-Prot.A was grown without or in the presence of 1 µg/ml doxycycline (DOX) and compared to strain RRN3-Prot.A (note that this is not the exact isogenic wild-type strain to pTet$_7$-RRN3-Prot.A). The culture was diluted to an OD600 of 0.1. After 6 h half of the culture was withdrawn and rapamycin was added to a final concentration of 200 ng/ml (indicated by an arrow). The OD600 of the culture was monitored hourly over the entire 10-h time-course of the experiment.

35S, 27S and 20S pre-rRNAs are equally diminished after doxycycline dependent Rrn3p-reduction. This is reflected in a constant quotient of newly synthesized 35S/27S rRNA (Figure 5C). Since processing defects generally lead to the distortion of the precursor rRNA ratios, we conclude that in this experiment Pol I transcription, but not rRNA processing is affected. We further investigated

the association of the Pol I subunit A43 with the promoter, 18S and 25S region of the rDNA in ChIP experiments in dependency of Rrn3p expression (Figure 5E). Doxycycline-dependent reduction of Rrn3p levels correlated well with a decrease in rDNA-associated Pol I. Taken together, our data demonstrate a correlation between Rrn3p levels, the formation of Rrn3p–Pol I

complexes, recruitment of Pol I to the rRNA genes, rRNA gene transcription and the growth rate in yeast.

In the presence of 0.2 µg/ml doxycycline the Rrn3p level in pTet$_7$-*RRN3-Prot.A* cells was very similar to the Rrn3p level in wild-type cells after 2 h of rapamycin treatment (Figure 5D, upper panel, compare lanes 3 and 4). Strikingly, we observed large differences in the pattern of newly synthesized (pre)-rRNA in these two conditions: As noted before (Figure 5C), doxycyline treatment affected the different precursors similarly, with no evidence for defective processing (Figure 5D, compare lane 4 with lane 1). After 20 min of rapamycin treatment Rrn3p levels did not drop significantly, but rRNA labelling and processing were strongly affected. [Note, that cellular uptake of uracil was only modestly affected after 20 min rapamycin treatment (data not shown, and Reiter *et al.*, submitted)]. Accordingly, substantial amounts of newly synthesized 35S pre-rRNA are still detected, whereas label incorporation in matured rRNA species was reduced in rapamycin treated cells [compare Figure 5D, lane 4 with lane 2/3; lane 1 with lane 2/3, and lane 4 with lane 5/6; see also (45)].

Furthermore, in contrast to the doxycycline-treated pTet$_7$-*RRN3-Prot.A* strain, rapamycin treated cultures stopped growth shortly after addition of the drug (Figure 5F). Rapamycin dependent growth arrest occurred with the same kinetics [about 1 h after addition of rapamycin (arrow in Figure 5F)], no matter whether Rrn3p was overexpressed or scarce (Figure 5F). Therefore, the simple reduction of Rrn3p-levels and consequently the decreased association of the Pol I-machinery with rDNA do not fully explain the dramatic effects on ribosome neo-production and cellular growth upon TOR inhibition.

DISCUSSION

Our analyses confirm that in yeast the complex control of ribosome biosynthesis occurs on several layers. One of them is the proteasome-dependent degradation of the transcription factor Rrn3p which contributes to the down-regulation of transcription initiation as a consequence of TOR inactivation by rapamycin. Several observations indicate that lowered cellular Rrn3p levels after TOR inactivation are not the result of a targeted destruction [see as review (47)], but rather the combination of a reduced RRN3 expression rate and a constitutive short half life of the protein (48): first, RRN3 mRNA levels quickly decrease upon nutrient depletion. [(38,49) and our results, not shown]. Second, both inactivation of Pol II-dependent transcription of the RRN3 gene in Pol II conditional mutant and inhibition of RRN3 mRNA translation by cycloheximide reduce Rrn3p protein levels with similar kinetics as TOR inactivation, thus, TOR inactivation affects endogenous Rrn3p levels very likely at the stage of or prior to protein production.

Ubiquitylation of Rrn3p seems to be an evolutionary conserved feature since this modification has recently been reported for the mammalian homologue, TIF-IA (50). However, in contrast to the endogenous yeast Rrn3p, TOR-inactivation does not lead to reduced levels of ectopically co-expressed TIF-IA in the mammalian system (12). Thus, it appears that—although human TIF-IA/Rrn3p substitutes the yeast homologue for growth (51)—their activities may be differently regulated. It is conceivable that the requirements to respond to incoming signals differ between a rapidly dividing yeast cell and higher eukaryotic cells which have more time to adjust to environmental situations.

Nomura and co-workers (11,40) reported that the TOR pathway regulates Rrn3p-dependent recruitment of Pol I to the rDNA. Using ChIP assays and EM Miller spreading technology they calculated that inhibition of the TOR pathway reduces the Pol I-coverage on the rDNA gene to about 40–50% of the normal levels (40) . In addition, they observed that the amount of Pol I associated with Rrn3p was reduced by a factor of about three after TOR inactivation by rapamycin (11). Our data suggest that decreasing cellular Rrn3p levels after TOR inactivation is one important cellular mechanism to reduce the amount of Pol I–Rrn3p complexes. On the other hand, in cells expressing a stabilized Rrn3p variant we still observed some reduction in the level of Pol I–Rrn3p complexes after nutrient depletion indicating that Rrn3p association with Pol I can also be regulated by other means. The kinase Tor1p was reported to be associated with the rDNA promoter in exponentially growing cells, whereas it shuttles to the cytoplasm upon TOR inactivation (52). Thus, it is possible that nuclear Tor1p directly modulates the formation and dissociation of the Pol I–Rrn3p complex.

Experiments using a non-dissociable Pol I–Rrn3p fusion protein (CARA for Constitutive Association of Rrn3 and A43) are in general agreement with our conclusions (25). The CARA strain mimics an active non-dissociable Pol I–Rrn3p complex, which is resistant to rapamycin treatment. Similar to the ΔN mutant analysed in this study this strain shows an attenuation of the rapamycin-dependent repression of transcription. However, the retention of Pol I at the rDNA upon rapamycin treatment is significantly higher in the CARA strain than in the ΔN mutant strain upon nutrient starvation [compare Figure 4C in this study with Figure 2B in (25)]. This is consistent with the interpretation, that in the CARA strain, both, the decrease in Rrn3p protein levels, and the Rrn3p-A43 dissociation are prevented. On the other hand, also in CARA expressing cells overall rRNA synthesis is substantially reduced upon rapamycin treatment (Figure 4D in (25)). This indicates the existence of other mechanisms regulating rRNA production independent of the formation of the Pol I–Rrn3p complex also in this experimental system.

If we adjust Rrn3p levels to values substantially below the reduced amounts of Rrn3p observed upon TOR inactivation by rapamycin, we find a significant reduction in rRNA synthesis. In contrast to TOR inactivation, however, mature rRNAs are still produced even if amounts of initiation competent Pol I–Rrn3p complexes are minimal. We conclude that nutrient dependent regulation of cellular Rrn3p levels alters rDNA transcription on the level of the (re-) initiation rate (11,42) but does not fully account for the TOR-dependent shut-down of

ribosome production. Delays in posttranscriptional steps of ribosome maturation after TOR inactivation, as indicated by the relative accumulation of the 35S rRNA precursor (Figures 4D and 5D) and the re-localization of certain ribosome biogenesis factors (53,54), could explain these obvious differences.

In conclusion, our work investigating the effects of Rrn3p level alterations has revealed that the endogenous Rrn3p level is a determinant for the formation of initiation competent Pol I–Rrn3p complexes, influencing the (re-)initiation rate at rRNA genes. Rrn3p levels can thus directly influence Pol I transcription, which may be important for long-term adjustment of ribosome synthesis. TOR inactivation also reduces Rrn3p levels but we provide clear evidence that this reduction cannot explain the dramatic decrease in mature rRNA production (Figure 5D). Accordingly, artificial down-regulation of Rrn3p slows down but does not inhibit cell growth, whereas TOR inactivation results in immediate growth arrest. This all supports the idea, that under certain physiological situations down-regulation of rRNA production can be uncoupled from efficient Pol I initiation complex formation. Therefore, a main target of TOR inactivation in yeast to quickly adjust ribosome biosynthesis to changes in environmental conditions is likely downstream of transcription initiation (see also Reiter *et al*., submitted).

SUPPLEMENTARY DATA

Supplementary Data are available at NAR Online.

ACKNOWLEDGEMENTS

FUNDING

REFERENCES

1. Russell,J. and Zomerdijk,J.C. (2005) RNA-polymerase-I-directed rDNA transcription, life and works. *Trends Biochem. Sci.*, **30**, 87–96.
2. Moss,T., Langlois,F., Gagnon-Kugler,T. and Stefanovsky,V. (2007) A housekeeper with power of attorney: the rRNA genes in ribosome biogenesis. *Cell. Mol. Life Sci.*, **64**, 29–49.
3. Grummt,I. (2003) Life on a planet of its own: regulation of RNA polymerase I transcription in the nucleolus. *Genes Dev.*, **17**, 1691–1702.
4. Heix,J., Vente,A., Voit,R., Budde,A., Michaelidis,T.M. and Grummt,I. (1998) Mitotic silencing of human rRNA synthesis: inactivation of the promoter selectivity factor SL1 by cdc2/cyclin B-mediated phosphorylation. *EMBO J.*, **17**, 7373–7381.
5. Klein,J. and Grummt,I. (1999) Cell cycle-dependent regulation of RNA polymerase I transcription: the nucleolar transcription factor UBF is inactive in mitosis and early G1. *Proc. Natl Acad. Sci. USA*, **96**, 6096–6101.
6. Stefanovsky,V.Y., Pelletier,G., Hannan,R., Gagnon-Kugler,T., Rothblum,L.I. and Moss,T. (2001) An immediate response of ribosomal transcription to growth factor stimulation in mammals is mediated by ERK phosphorylation of UBF. *Mol. Cell.*, 8, 1063–1073.
7. Stefanovsky,V.Y., Langlois,F., Bazett-Jones,D., Pelletier,G. and Moss,T. (2006) ERK modulates DNA bending and enhancesome structure by phosphorylating HMG1-boxes 1 and 2 of the RNA polymerase I transcription factor UBF. *Biochemistry*, **45**, 3626–3634.
8. Zhao,J., Yuan,X., Frodin,M. and Grummt,I. (2003) ERK-dependent phosphorylation of the transcription initiation factor TIF-IA is required for RNA polymerase I transcription and cell growth. *Mol. Cell.*, **11**, 405–413.
9. Hannan,K.M., Brandenburger,Y., Jenkins,A., Sharkey,K., Cavanaugh,A., Rothblum,L., Moss,T., Poortinga,G., McArthur,G.A., Pearson,R.B. *et al.* (2003) mTOR-dependent regulation of ribosomal gene transcription requires S6K1 and is mediated by phosphorylation of the carboxy-terminal activation domain of the nucleolar transcription factor UBF. *Mol. Cell. Biol.*, **23**, 8862–8877.
10. James,M.J. and Zomerdijk,J.C. (2004) Phosphatidylinositol 3-kinase and mTOR signaling pathways regulate RNA polymerase I transcription in response to IGF-1 and nutrients. *J. Biol. Chem.*, **279**, 8911–8918.
11. Claypool,J.A., French,S.L., Johzuka,K., Eliason,K., Vu,L., Dodd,J.A., Beyer,A.L. and Nomura,M. (2004) Tor pathway regulates Rrn3p-dependent recruitment of yeast RNA polymerase I to the promoter but does not participate in alteration of the number of active genes. *Mol. Biol. Cell.*, **15**, 946–956.
12. Mayer,C., Zhao,J., Yuan,X. and Grummt,I. (2004) mTOR-dependent activation of the transcription factor TIF-IA links rRNA synthesis to nutrient availability. *Genes Dev.*, **18**, 423–434.
13. Mayer,C., Bierhoff,H. and Grummt,I. (2005) The nucleolus as a stress sensor: JNK2 inactivates the transcription factor TIF-IA and down-regulates rRNA synthesis. *Genes Dev.*, **19**, 933–941.
14. Voit,R., Schnapp,A., Kuhn,A., Rosenbauer,H., Hirschmann,P., Stunnenberg,H.G. and Grummt,I. (1992) The nucleolar transcription factor mUBF is phosphorylated by casein kinase II in the C-terminal hyperacidic tail which is essential for transactivation. *EMBO J.*, **11**, 2211–2218.
15. Hannan,R.D., Hempel,W.M., Cavanaugh,A., Arino,T., Dimitrov,S.I., Moss,T. and Rothblum,L. (1998) Affinity purification of mammalian RNA polymerase I. Identification of an associated kinase. *J. Biol. Chem.*, **273**, 1257–1267.
16. Panova,T.B., Panov,K.I., Russell,J. and Zomerdijk,J.C. (2006) Casein kinase 2 associates with initiation-competent RNA polymerase I and has multiple roles in ribosomal DNA transcription. *Mol. Cell. Biol.*, **26**, 5957–5968.
17. Stefanovsky,V., Langlois,F., Gagnon-Kugler,T., Rothblum,L.I. and Moss,T. (2006) Growth factor signaling regulates elongation of RNA polymerase I transcription in mammals via UBF phosphorylation and r-chromatin remodeling. *Mol. Cell.*, **21**, 629–639.
18. Panov,K.I., Friedrich,J.K., Russell,J. and Zomerdijk,J.C. (2006) UBF activates RNA polymerase I transcription by stimulating promoter escape. *EMBO J.*, **25**, 3310–3322.
19. Schawalder,S.B., Kabani,M., Howald,I., Choudhury,U., Werner,M. and Shore,D. (2004) Growth-regulated recruitment of the essential yeast ribosomal protein gene activator Ifh1. *Nature*, **432**, 1058–1061.
20. Wade,J.T., Hall,D.B. and Struhl,K. (2004) The transcription factor Ifh1 is a key regulator of yeast ribosomal protein genes. *Nature*, **432**, 1054–1058.

21. Martin,D.E., Soulard,A. and Hall,M.N. (2004) TOR regulates ribosomal protein gene expression via PKA and the Forkhead transcription factor FHL1. *Cell*, **119**, 969–979.
22. Wullschleger,S., Loewith,R. and Hall,M.N. (2006) TOR signalling in growth and metabolism. *Cell*, **124**, 471–484.
23. Moss,T. and Stefanovsky,V.Y. (2002) At the center of eukaryotic life. *Cell*, **109**, 545–548.
24. Milkereit,P. and Tschochner,H. (1998) A specialized form of RNA polymerase I, essential for initiation and growth dependent regulation of rRNA synthesis, is disrupted during transcription. *EMBO J.*, **17**, 3692–3703.
25. Laferte,A., Favry,E., Sentenac,A., Riva,M., Carles,C. and Chedin,S. (2006) The transcriptional activity of RNA polymerase I is a key determinant for the level of all ribosome components. *Genes Dev.*, **20**, 2030–2040.
26. Schmitt,M.E., Brown,T.A. and Trumpower,B.L. (1990) A rapid and simple method for preparation of RNA from Saccharomyces cerevisiae. *Nucleic Acids Res.*, **18**, 3091–3092.
27. Hecht,A. and Grunstein,M. (1999) Mapping DNA interaction sites of chromosomal proteins using immunoprecipitation and polymerase chain reaction. *Methods Enzymol.*, **304**, 399–414.
28. Leger-Silvestre,I., Milkereit,P., Ferreira-Cerca,S., Saveanu,C., Rousselle,J.C., Choesmel,V., Guinefoleau,C., Gas,N. and Gleizes,P.E. (2004) The ribosomal protein Rps15p is required for nuclear exit of the 40S subunit precursors in yeast. *EMBO J.*, **23**, 2336–2347.
29. Rozijn,T.H. and Tonino,G.J. (1964) Studies on the yeast nucleus. I. The tsolation of nuclei. *Biochim Biophys. Acta*, **91**, 105–112.
30. Merz,K., Hondele,M., Goetze,H., Gmelch,K., Stoeckl,U. and Griesenbeck,J. (2008) Actively transcribed rRNA genes in S. cerevisiae are organized in a specialized chromatin associated with the high-mobility group protein Hmo1 and are largely devoid of histone molecules. *Genes Dev.*, **22**, 1190–1204.
31. Osheim,Y.N., French,S.L., Sikes,M.L. and Beyer,A.L. (2009) Electron microscope visualization of RNA transcription and processing in Saccharomyces cerevisiae by Miller chromatin spreading. *Methods Mol. Biol.*, **464**, 55–69.
32. Yuan,X., Zhao,J., Zentgraf,H., Hoffmann-Rohrer,U. and Grummt,I. (2002) Multiple interactions between RNA polymerase I, TIF-IA and TAFI subunits regulate preinitiation complex assembly at the ribosomal gene promoter. *EMBO Rep.*, **3**, 1082–1087.
33. Cavanaugh,A.H., Hirschler-Laszkiewicz,I., Hu,Q., Dundr,M., Smink,T., Misteli,T. and Rothblum,L.I. (2002) Rrn3 phosphorylation is a regulatory checkpoint for ribosome biogenesis. *J. Biol. Chem.*, **277**, 27423–27432.
34. Hirschler-Laszkiewicz,I., Cavanaugh,A., Mizra,A., Lun,M., Hu,Q., Smink,T. and Rothblum,L.I. (2003) Rrn3 becomes inactivated in the process of ribosomal DNA transcription. *J. Biol. Chem.*, **278**, 18953–18959.
35. Rubin,D.M., Coux,O., Wefes,I., Hengartner,C., Young,R.A., Goldberg,A.L. and Finley,D. (1996) Identification of the gal4 suppressor Sug1 as a subunit of the yeast 26S proteasome. *Nature*, **379**, 655–657.
36. Gerlinger,U.M., Guckel,R., Hoffmann,M., Wolf,D.H. and Hilt,W. (1997) Yeast cycloheximide-resistant crl mutants are proteasome mutants defective in protein degradation. *Mol. Biol. Cell.*, **8**, 2487–2499.
37. Funakoshi,M., Sasaki,T., Nishimoto,T. and Kobayashi,H. (2002) Budding yeast Dsk2p is a polyubiquitin-binding protein that can interact with the proteasome. *Proc. Natl Acad. Sci. USA*, **99**, 745–750.
38. Huang,J., Zhu,H., Haggarty,S.J., Spring,D.R., Hwang,H., Jin,F., Snyder,M. and Schreiber,S.L. (2004) Finding new components of

the target of rapamycin (TOR) signaling network through chemical genetics and proteome chips. *Proc. Natl Acad. Sci. USA*, **101**, 16594–16599.
39. Bier,M., Fath,S. and Tschochner,H. (2004) The composition of the RNA polymerase I transcription machinery switches from initiation to elongation mode. *FEBS Lett.*, **564**, 41–46.
40. Oakes,M.L., Siddiqi,I., French,S.L., Vu,L., Sato,M., Aris,J.P., Beyer,A.L. and Nomura,M. (2006) Role of histone deacetylase Rpd3 in regulating rRNA gene transcription and nucleolar structure in yeast. *Mol. Cell. Biol.*, **26**, 3889–3901.
41. McKnight,S.L. and Miller,O.L. Jr (1976) Ultrastructural patterns of RNA synthesis during early embryogenesis of Drosophila melanogaster. *Cell*, **8**, 305–319.
42. French,S.L., Osheim,Y.N., Cioci,F., Nomura,M. and Beyer,A.L. (2003) In exponentially growing Saccharomyces cerevisiae cells, rRNA synthesis is determined by the summed RNA polymerase I loading rate rather than by the number of active genes. *Mol. Cell. Biol.*, **23**, 1558–1568.
43. Conconi,A., Widmer,R.M., Koller,T. and Sogo,J.M. (1989) Two different chromatin structures coexist in ribosomal RNA genes throughout the cell cycle. *Cell*, **57**, 753–761.
44. Dammann,R., Lucchini,R., Koller,T. and Sogo,J.M. (1993) Chromatin structures and transcription of rDNA in yeast Saccharomyces cerevisiae. *Nucleic Acids Res.*, **21**, 2331–2338.
45. Powers,T. and Walter,P. (1999) Regulation of ribosome biogenesis by the rapamycin-sensitive TOR-signaling pathway in Saccharomyces cerevisiae. *Mol. Biol. Cel.l*, **10**, 987–1000.
46. Gari,E., Piedrafita,L., Aldea,M. and Herrero,E. (1997) A set of vectors with a tetracycline-regulatable promoter system for modulated gene expression in Saccharomyces cerevisiae. *Yeast*, **13**, 837–848.
47. Muratani,M. and Tansey,W.P. (2003) How the ubiquitin-proteasome system controls transcription. *Nat. Rev. Mol. Cell. Biol.*, **4**, 192–201.
48. Belle,A., Tanay,A., Bitincka,L., Shamir,R. and O'Shea,E.K. (2006) Quantification of protein half-lives in the budding yeast proteome. *Proc. Natl Acad. Sci. USA*, **103**, 13004–13009.
49. Jorgensen,P., Rupes,I., Sharom,J.R., Schneper,L., Broach,J.R. and Tyers,M. (2004) A dynamic transcriptional network communicates growth potential to ribosome synthesis and critical cell size. *Genes Dev.*, **18**, 2491–2505.
50. Fatyol,K. and Grummt,I. (2008) Proteasomal ATPases are associated with rDNA: the ubiquitin proteasome system plays a direct role in RNA polymerase I transcription. *Biochim Biophys Acta*, **1779**, 850–859.
51. Moorefield,B., Greene,E.A. and Reeder,R.H. (2000) RNA polymerase I transcription factor Rrn3 is functionally conserved between yeast and human. *Proc. Natl Acad. Sci. USA*, **97**, 4724–4729.
52. Li,H., Tsang,C.K., Watkins,M., Bertram,P.G. and Zheng,X.F. (2006) Nutrient regulates Tor1 nuclear localization and association with rDNA promoter. *Nature*, **442**, 1058–1061.
53. Honma,Y., Kitamura,A., Shioda,R., Maruyama,H., Ozaki,K., Oda,Y., Mini,T., Jeno,P., Maki,Y., Yonezawa,K. *et al.* (2006) TOR regulates late steps of ribosome maturation in the nucleoplasm via Nog1 in response to nutrients. *EMBO J.*, **25**, 3832–3842.
54. Vanrobays,E., Leplus,A., Osheim,Y.N., Beyer,A.L., Wacheul,L. and Lafontaine,D.L. (2008) TOR regulates the subcellular distribution of DIM2, a KH domain protein required for cotranscriptional ribosome assembly and pre-40S ribosome export. *RNA*, **14**, 2061–2073.